*Selected papers presented at the 14th Symposium of Magnetic Measurements and Modelling SMMM'2023*

# Are There Any Alternatives for Rare-Earth Permanent Magnets?

M.F. de Campos*

*Federal Fluminense University (UFF), Av. dos Trabalhadores 420 Volta Redonda RJ, 27255-125 Brazil*

Doi: 10.12693/APhysPolA.146.26 *e-mail: marcosflavio@id.uff.br

Iron-based rare-earth permanent magnets are in high demand due to a large number of their applications, including electric cars and cell phones. Alternatives to rare-earth permanent magnets are discussed. Hard ferrites appear to be the simplest option for the replacement of rare-earth magnets due to their easy processing and low cost. The possibilities of replacing NdPrFeB magnets are discussed on the basis of the Bethe–Slater curve. Instead of developing alternatives to rare-earth magnets, research should focus on cheap production of Nd and Pr.

topics: permanent magnets, ferrite magnets, rare-earth magnets, Bethe–Slater curve

## 1. Introduction

Rare-earth permanent magnets are essential in many applications, for example, motors of electric cars [1], which may use 1–2 kg of NdFeB-type magnets per vehicle. These magnets are described by the stoichiometric formula $RE_2Fe_{14}B$, where RE (rare-earth) element is neodymium or praseodymium, and terbium or dysprosium can be added to increase the operation temperature. NdFeB magnets are also extensively used in loudspeakers of cell phones and in hard-disk motors [2]. The large number of applications has led to a large increase in demand, which has driven up the price of rare-earth elements Nd, Pr, Dy, and Tb.

Reports by the U.S. government [3] and the European Union [4, 5] indicate that electric vehicles and off-shore wind turbines can significantly increase the demand for rare-earth permanent magnets in the forthcoming years.

The present study discusses possible alternatives to rare-earth magnets of the REFeB family. Possible ferromagnetic compounds are discussed on the basis of the Bethe–Slater curve. From this analysis, RE–Fe alloys with nitrogen or Mn-based alloys with aluminum or bismuth appear to be good candidates. However, phase instability problems preclude large-scale commercial utilization of SmFeN or MnAl compounds.

SmCo-based magnets use cobalt, which is in high demand due to a large number of applications, such as batteries in electric cars. Therefore, cobalt-based magnets are not an option for replacement of NdFeB magnets due to the high price of cobalt.

The most clear alternatives for NdFeB are barium and strontium ferrite magnets, which have the formula $BaFe_{12}O_{19}$ or $SrFe_{12}O_{19}$. These magnets are oxides and have very simple processing. Whereas ferrite magnets are in the range of 3–7 US$/kg [6, 7], NdFeB magnets are at 50 US$/kg or more. Thus, although the maximum energy product of ferrite magnets is 10% of NdFeB, ferrite magnets are an option when there is no volume limitation. As ferrites are oxides, they have low resistivity and can be an interesting option in rotating machines.

Ores containing Pr and Nd, for example, monazite, are very abundant around the world. Thus, Nd and Pr can become cheap thanks to better technologies for concentrating rare-earth elements from ore, as well as improving rare-earth oxide separation methods [8, 9] for magnet manufacture.

## 2. Rare-earth elements

Rare-earth elements are not particularly rare, but they were first identified in an ore from Ytterby (Sweden) [10], which was considered rare at that time. Earth was the name given to the calcinated residues in the late XVIII century. Rare-earth elements are not very common in Europe, but as a phosphate monazite $REPO_4$, they are found in many parts of the world [11], for example, on the shores of Brazil and the United States [12] as monazite sand. Some rare-earth minerals, such as monazite and xenotime, have also a significant amount of thorium and uranium. Uranium has applications

TABLE I

Rare-earth proportion in some possible mining sites in Brazil compared with the Mountain Pass Mine in California, USA.

| | CBMM Araxa (Minas Gerais) monazite | Morro do Ferro Poços de Caldas (Minas Gerais) monazite | Serra Verde (Goiás) ionic clay | Pitinga (Amazonas) xenotime | Caldeira Poços de Caldas (Minas Gerais) ionic clay | Mountain Pass (California, USA) bastnaesite |
|---|---|---|---|---|---|---|
| $La_2O_3$ | 30.6 | 26.6 | 32.1 | 0.5 | 46.8 | 33.79 |
| $CeO_2$ | 44.1 | 48.7 | 4.2 | 5.0 | 18.3 | 49.59 |
| $Pr_6O_{11}$ | 4.6 | 5.0 | 5.9 | 0.7 | 6.5 | 4.12 |
| $Nd_2O_3$ | 15.3 | 13.7 | 19.3 | 2.2 | 17.9 | 11.16 |
| $Sm_2O_3$ | 1.58 | 1.5 | 3.3 | 1.9 | 2.0 | 0.85 |
| $Eu_2O_3$ | 0.38 | 0.4 | 0.2 | 0.2 | 0.5 | 0.105 |
| $Gd_2O_3$ | 1.28 | 0.9 | 3.2 | 4.0 | 1.4 | 0.21 |
| $Tb_4O_7$ | 0.12 | 0.1 | 0.5 | 1.0 | 0.2 | 0.016 |
| $Dy_2O_3$ | 0.42 | 0.5 | 3.2 | 8.7 | 0.8 | 0.034 |
| $Ho_2O_3$ | 0.06 | 0.1 | 0.7 | 2.1 | 0.1 | 0.004 |
| $Er_2O_3$ | 0.15 | 0.2 | 2.0 | 5.4 | 0.3 | 0.006 |
| $Tm_2O_3$ | 0.01 | – | 0.3 | 0.9 | 0 | 0.002 |
| $Yb_2O_3$ | 0.06 | 0.2 | 1.8 | 6.2 | 0.3 | 0.002 |
| $Lu_2O_3$ | 0.01 | 0.02 | 0.3 | 0.4 | 0 | $< 0.01$ |
| $Y_2O_3$ | 1.29 | 2.0 | 23.0 | 60.8 | 4.7 | $< 0.13$ |

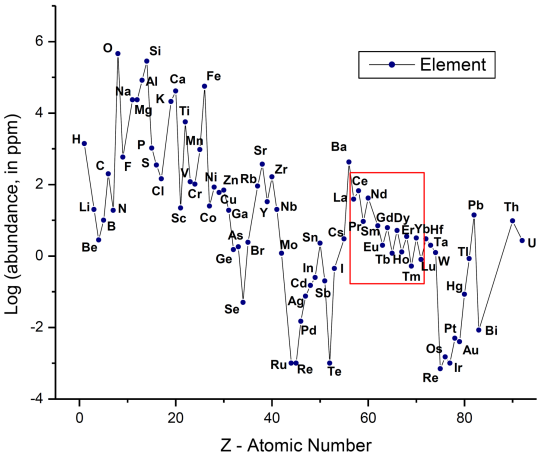


Fig. 1. Abundance of elements in the crust of Earth. In the red box — a lanthanide series. Elements with odd atomic numbers are less abundant, which confirms the Oddo–Harkinks rule.

in nuclear plants, but thorium has virtually no applications, and thorium disposal is usually a significant and expensive problem.

Figure 1 was constructed from data provided by Lide [13]. Light rare earths (Ce, La, Pr, and Nd) are abundant, but heavy rare-earth elements such as Tb, Ho, and Eu are scarce. This is reflected in the ores, as can be seen in Table I. The data in Table I was presented in a previous study [14], and now it is updated with data from the Caldeira project in Poços de Caldas (Minas Gerais, Brazil) [15]. For comparison, data from the Mountain Pass mine near Las Vegas in the United States [16] is also included. After the bankruptcy of the Mountain Pass mine in 2015 [17], many rare-earth mining projects

TABLE II

Polarization of saturation, anisotropy field, and Curie temperature of 2:14:1 compounds.

| | $J_s$ [T] | $\mu_0 H_A$ [T] | $T_C$ [°C] | Ratio $\mu_0 H_A / J_s$ |
|---|---|---|---|---|
| Y | 1.41 | 2.0 | 298 | 1.4 |
| Ce | 1.17 | 2.6 | 150 | 2.2 |
| Pr | 1.56 | 8.7 | 296 | 5.6 |
| Nd | 1.6 | 7.7 | 312 | 4.8 |
| Gd | 0.89 | 2.5 | 387 | 2.8 |
| Tb | 0.70 | 22 | 347 | 31.4 |
| Dy | 0.71 | 15 | 325 | 21,1 |
| Ho | 0.81 | 7.5 | 300 | 9.3 |

in Brazil were either postponed or canceled. Many projects have been announced in Brazil recently, i.e., in 2023, aiming at the extraction of rare-earth elements from the ionics clays. Deposits containing ionic clays have gained much attention recently [18], and one of the reasons is the larger amount of heavy rare-earth elements, as can be seen in Table I. In contrast, the Mountain Pass bastnaesite mine has only traces of dysprosium and terbium (see Table I). It can also be observed in Table I that most of the ores contain Pr and Nd in an approximate proportion of 1:3, confirming the Oddo–Harkins rule [19]. Nd and Pr are not usually separated in the production of a magnet, and this alloy is commercially available under the name didymium. The separation of neodymium and praseodymium is a very difficult task due to the chemical similarities between these elements [20–24].

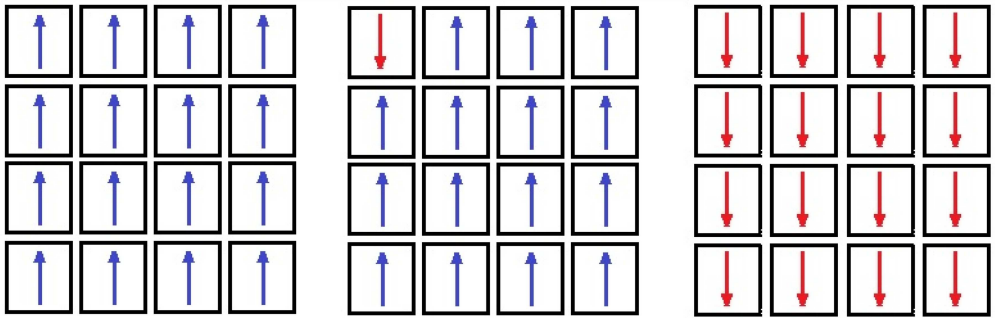

Fig. 2. Chain effect. Reversal of magnetization in a given grain provokes a chain or cascade effect, with the inversion of the magnetization in the neighbor grains. A high ratio $\mu_0 H_A/J_s$ avoids the chain effect.

TABLE III

Chemical composition of some magnets found in motors of electric vehicles, according to S. Munro [35].

| | Tesla Model 3 magnet | "standard automotive magnet" |
|---|---|---|
| Dy | 1.19 | 3.47 |
| Nd | 23.01 | 19.90 |
| Pr | 7.70 | 6.67 |
| Sm | 1.42 | 0.86 |
| Fe | 57.38 | 62.51 |
| Co | 1.72 | 1.79 |
| Cu | 2.11 | 1.10 |
| Al | 0.96 | 1.37 |
| O | 4.50 | 2.33 |

Table II was compiled on the basis of several sources [25–30]. The three most relevant intrinsic properties are $T_C$ — Curie temperature, $J_s$ — polarization of saturation, $H_A$ — anisotropy field, and $M_s$ — magnetization of saturation. Dy, Ho, and Gd are commercially available as ferroalloys, and the only explanation for this is that they are used as alloying elements in NdPrFeB magnets. Alloying iron reduces the melting temperature, making it easier to obtain Fe–Dy, Fe–Gd, and Fe–Ho rather than the pure metals Dy, Ho, and Gd. Dysprosium and terbium are essential for increasing the operation temperature in NdPrFeB magnets. Holmium is a cheap alternative to dysprosium. Gd increases the Curie temperature, as can be seen in Table II, but it significantly reduces the anisotropy field, and thus, the Gd addition is used in the cheaper grades. The addition of cerium has some significant problems as it reduces both $T_C$ and $H_A$, i.e., Ce reduces the operation temperature and coercivity. Also, because Ce has a lower magnetization of saturation, it "dilutes" the magnetic moment, and this implies a larger volume of the magnet. In conclusion, cerium-based magnets cannot compete with barium or strontium magnets because they would be very expensive given the similar properties of ferrites at room temperature.

TABLE IV

Magnet mass per motor of electric vehicle.

| Vehicle | Magnet mass [kg] |
|---|---|
| Honda Accord M | 0.755 |
| Honda Accord G | 1.24 |
| Nissan Leaf | 1.895 |
| Toyota Prius 2010 | 0.768 |
| Toyota Prius 2004 | 1.232 |
| Lexus LS 600h | 1.349 |
| Toyota Camry | 0.928 |
| Toyota Prius 2017 | 0.544 |
| BMW i3 2016 | 2 |
| Tesla Model 3 | 1.783 |
| Jaguar I-PACE | 1.85 |
| Volkswagen ID.3 | 2.5 |
| Chevrolet Volt | 1.57 |

The non-written rule is that the anisotropy field should be well above saturation to avoid a chain effect. For example, the ratio $\mu_0 H_A/J_s$ for $Nd_2Fe_{14}B$ is 4.8 (see Table II). It is very difficult to find phases with such high ratios. One of them are the $BaFe_{12}O_{19}$ ferrites, with $H_A = 16$ kOe [31] and $M_s = 4.8$ kG [32], where such ratio is 3.3 and also $T_C = 450$°C. In addition to the chain effect [33] exemplified in Fig. 2, grain size is another very relevant variable. The grain should be the size of a single domain. Thus, melt-spinning is a common practice used for hard magnetic materials to obtain nanocrystalline magnets. Another possibility is shape anisotropy [34], which allows the use of even very soft phases as hard magnetic materials.

Munro [35] mentioned the chemical composition of magnets used in electric vehicles. It is observed in Table III that such a magnet has a 1:3 Pr/Nd proportion and contains some dysprosium (and not Ho, Gd, or Ce). Table IV is an update of the table of a previously presented study [36]. Table IV shows that the electric vehicle industry has a clear preference for motors with magnets in the rotor. This saves energy and increases motor efficiency,

resulting in increased autonomy of the electric car. However, high-efficiency motors without magnets are possible, as in the old Tesla Model S and Audi e-tron [37]. General Motors Company (GM) tried a motor with ferrite in the 2015 Chevrolet Volt [38], but gave preference for NdFeB-type in later versions[†1]. Motors with ferrite-based rotors are less efficient than those with NdFeB-based rotors [39, 40].

In many designs, the magnets are inserted in the rotor following a "double V" topology [41], which allows for a reduction of the cogging torque [42], a typical problem at low speeds. Tesla made a significant innovation with the carbon-wrapped rotor [43], enabling the elimination of the radial and tangential iron ribs of the rotor, thus avoiding problems of magnetic flux leakage [44, 45]. These high-efficiency designs in general request NdFeB-type magnets, using 0.5–2.5 kg of magnets per motor, as can be seen in Table IV.

Also, wind turbines request NdFeB-type magnets, especially for giant off-shore turbines [46, 47]. Thus, the question is about the possibility of replacing rare-earth magnets with other types of magnets. Although some elements are truly scarce, such as terbium and dysprosium, light rare-earth elements such as Nd and Pr are very common, and monazite, for example, is a very common ore, found in almost the entire world. Thus, research should be directed towards cheaper production methods for Nd and Pr, as well as avoiding Tb and Dy, and this can be obtained with better designs that allow lower operation temperatures.

## 3. Alternatives for rare-earth permanent magnets

Before discussing possible phases, it is worth adding that a relevant hint can be given by the Stoner–Wohlfarth (SW) model [48]. The energy $E$ is here

$$E = -HM_s\cos(\theta-\alpha) + K_1\sin^2(\theta), \tag{1}$$

where $K_1$ is the magnetocrystalline anisotropy. The angle between the external field $H$ and the crystal easy axis is $\alpha$. The angle between $M_s$ and the easy axis is $\theta$. By making $\mathrm{d}E/\mathrm{d}\theta = 0$ and $\mathrm{d}^2E/\mathrm{d}\theta^2 = 0$, the critical field $h_c$ for irreversible rotation is obtained as

$$h_c = \frac{(1-t^2+t^4)^{1/2}}{1+t^2}, \tag{2}$$

and it is a function of $t$, where $t$ relates to $\alpha$ by [49]

$$t = (\tan(\alpha))^{1/3}. \tag{3}$$

[†1]Chevrolet gave similar names for different vehicles; Chevrolet Volt is a hybrid, whereas Bolt is a full battery car.

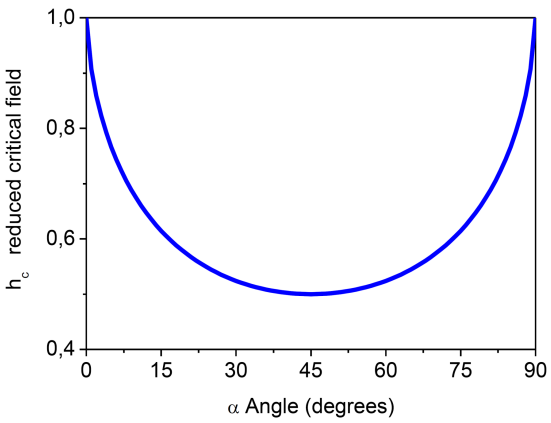


Fig. 3. Reduced field $h_c$ as a function of angle $\alpha$. According to the Stoner–Wohlfarth (SW) model, there are regions of reversible and irreversible rotation. For $-0.5 \le h_c \le 0.5$, there is always reversible rotation.

TABLE V

Polarization of saturation and anisotropy field for hard ferrites, Mn-based compounds, and nitrogen-related compounds.

| | Reference | $J_s$ [T] | $\mu_0 H_A$ [T] | Ratio $\mu_0 H_A/J_s$ |
|---|---|---|---|---|
| MnAl | [50] | 0.62 | 4.0 | 6.4 |
| MnBi | [50] | 0.78 | 3.7 | 4.7 |
| $BaFe_{12}O_{19}$ | [50, 51] | 0.48 | 1.6 | 3.4 |
| $SrFe_{12}O_{19}$ | [50, 51] | 0.46 | 1.95 | 4.3 |
| $\alpha''$-$Fe_{16}N_2$ | [52] | 2.68 | 1.7 | 0.6 |
| $Sm_2Fe_{17}N_3$ | [53] | 1.54 | 14 | 9.1 |

According to Fig. 3, a useful criterion is that the suitable phases for permanent magnets should fulfill $\mu_0 H_A/J_s > 2$ to avoid the chain effect. This limits considerably the possible candidate phases.

Table V was constructed mainly based on data from Luborsky [50], and the anisotropy values for Ba and Sr ferrites were recently determined [51] to be very close to the values reported by Luborsky [50]. Also, data for nitrogen compounds $\alpha''$-$Fe_{16}N_2$ [52] and $Sm_2Fe_{17}N_3$ [53] are also included in Table V. It is observed in Table V that the manganese compounds MnAl and MnBi are appearing as possibilities for replacing hard ferrites. Thus, among other possible candidates to replace NdFeB and ferrites, the main other families are [54] $Fe_{16}N_2$, MnAl and MnBi, and $Sm_2Fe_{17}N_x$ magnets, because a high anisotropy field is an essential condition. Again, it is worth recalling the criterion $\mu_0 H_A/J_s > 2$, and this criterion is satisfied by $Sm_2Fe_{17}N_x$, MnBi, and MnAl. The permanent magnet market in 2022 [55] shown in Table VI, in addition to ferrites and NdFeB, only mentions Alnico and SmCo.

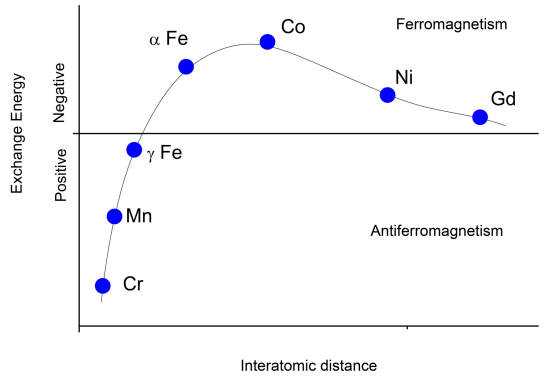


Fig. 4. The Bethe–Slater curve. Scheme based on Hosford [58].

TABLE VI

Percentage of the 23 US$ billion world permanent magnet market in 2022 [55].

| Type of magnet | % of the market |
|---|---|
| sintered NdFeB | 58% |
| bonded NdFeB | 6% |
| sintered ferrite | 26% |
| flexible ferrite | 4% |
| injection molded ferrite | 3% |
| SmCo | 1% |
| Alnico | 1% |
| others | 1% |

According to data in Table VI, only NdFeB and ferrites are disputing the market. The reason is simple, namely ferrite is very cheap, and other materials can not compete in terms of cost. Alnico has some niche applications, essentially sensors, and SmCo 2:17 has some high-temperature applications. $SmCo_5$ has been almost completely replaced by SmCo 2:17, i.e., SmCoFeCuZr. The fluctuation of cobalt price also precludes a larger usage of Co-based magnets such as SmCo 2:17, $SmCo_5$, and Alnico. In $SmCo_5$ magnets, 2/3 of the weight is cobalt. As can be seen in Table VI, Alnico is the only commercial magnet with a coercivity mechanism due to shape anisotropy [56, 57].

Figure 4 is based on the Hosford version [58] of the Bethe–Slater curve. It is semi-empirical, but it is still used for the interpretation of experimental results [59]. The Bethe–Slater curve is considered to be able to explain why stainless steels are not ferromagnetic. For example, the interatomic distance in FCC iron is smaller: for BCC iron — PF = 0.68, for FCC iron — PF = 0.74, where PF = packing factor. It follows that stainless steel 304 with 18% Cr and 8% Ni is not ferromagnetic.

Essentially, it is suggested in Fig. 4 that increasing the separation between Fe atoms and between Mn atoms can make them ferromagnetic. In manganese-based alloys, this is achieved by alloying Mn with large atoms: Bi, Al, and Ga. For iron-based alloys, this is achieved by using interstitial elements, such as boron or nitrogen. Thus, all suggestions by the Bether-Slater curve were already exploited experimentally. Heusler alloys are ferromagnetic, but their alloying elements were diamagnetic or paramagnetic, as can be seen in the classical $Cu_2MnAl$ composition [60]. The Bether–Slater curve also suggests rare-earth compounds, as can be noted from the presence of gadolinium in Fig. 4.

However, to be permanent magnet, the candidate phase needs to have high magnetocrystalline anisotropy in addition to ferromagnetism itself. Besides, the phase diagram is decisive, and so metastable phases are usually not suitable for commercial application due to lack of reproducibility.

The commercial production of Mn-based alloys has several problems: corrosion [61], metastable phases [62], and difficult processing. In 1980, MnAlC was commercially available from Matsushita, but its properties were hardly comparable with Alnico magnets and had the drawback of expensive processing [63]. The recoil curves presented by Abdelnour et al. [63] are similar to others found in SmCo 2:17 magnets [64], SmCoCu [65], and barium ferrites [31] — and this implies that all of them are the single domain size. This characteristic is essential and explains why many studies employ melt-spinning. The reason is obtaining single-domain particle size because this is a condition that allows to maximize the coercivity.

Approximately 60 years ago, the Phillips Company did intense research to develop commercial MnAl and MnBi magnets [62], reporting for MnAl coercivity up to 6 kOe. However, in MnAl alloys, the magnetic phase is metastable, and manganese alloys oxidize easily, making the production of magnets very difficult.

Lodex was a material that used the principle of shape anisotropy [32]. It was commercially available but had a coercivity of only $\sim$ 1 kOe [66]. Daido Steel has a bonded magnet made with melt-spun $Sm_2Fe_{17}Nx$ alloy in the catalog. A typical problem in nitrogen-based alloys is the lack of reproducibility. The nitrogen expands the lattice. To reduce internal stresses, the nitrogen atoms are expelled. Thus, phase instability is a significant issue in nitrogen magnetic alloys.

As almost all the possibilities given by the Bethe–Slater curve [67–69] were already tested, replacing NdFeB or barium and strontium ferrites is indeed a very difficult task.

## 4. Conclusions

It is difficult to find permanent magnetic materials that can compete with ferrites (cost) or NdFeB (performance). SmCo and Alnico still have

some niche applications. These are the principal 4 families of commercial permanent magnets. The other main candidates are or were commercially available.

Lodex and MnAlC were manufactured commercially. SmFeN is also manufactured commercially. However, these alternatives have problems competing with traditional materials: Alnico, SmCo, and especially ferrites and NdFeB. For a rare-earth free phase to be able to compete with ferrites, it is necessary that it has at least 50% higher $H_A$ and 50% $M_s$ than Sr and Ba ferrites. Except for MnBi and MnAl, such materials do not exist.

The Bether–Slater curve provides suggestions for phases that can be used as permanent magnets. But these suggestions were also exhausted.

Instead of researching new materials to replace NdPrFeB magnets, research should focus on cheap production of Nd and Pr. There are immense deposits of monazite in the world, containing significant amounts of Nd and Pr. Terbium and dysprosium, on the other hand, will always be scarce and expensive.

The ratio $\mu_0 H_A/J_s$ is suggested as a tool to evaluate the possibility of a given phase to be a candidate for a permanent magnet. The criterion is $\mu_0 H_A/J_s > 2$ to avoid the chain or cascade effect.

## Acknowledgments

The author thanks Fundação de Amparo à Pesquisa do Estado do Rio de Janeiro) (FAPERJ) and Conselho Nacional de Desenvolvimento Científico e Tecnológico (CNPq).

## References

[1] G. Zorpette, "What Is Tesla's Mystery Magnet?" *IEEE Spectrum* (2023).

[2] X. Lim "Global Initiative Mines Retired Hard Disk Drives for Materials and Magnets" *IEEE Spectrum* (2019).

[3] B.J. Smith, M.E. Riddle, M.R. Earlam, C. Iloeje, D. Diamond, *Rare Earth Permanent Magnets: Supply Chain Deep Dive Assessment*, U.S. Department of Energy, 2022.

[4] P. Alves Dias, S. Bobba, S. Carrara, B. Plazzotta, *The Role of Rare Earth Elements in Wind Energy and Electric Mobility*, EUR 30488 EN, Publications Office of the European Union, Luxembourg 2020, JRC122671.

[5] S. Carrara, S. Bobba, D. Blagoeva et al., *Supply Chain Analysis and Material Demand Forecast in Strategic Technologies and Sectors in the EU – A Foresight Study*, Publications Office of the European Union, Luxembourg 2023, JRC132889.

[6] M.F. de Campos, D. Rodrigues, J.A. de Castro, *Mater. Sci. Forum* **912**, 106 (2018).

[7] J. McKenzie, "Powering the Green Economy: The Guest for Magnets without Rare Earths", Physics World, 2023.

[8] S.V.S.H. Pathapati, M.L. Free, P.K. Sarswat, *Processes* **11**, 2070 (2023).

[9] M. Traore, A. Gong, Y. Wang et al., *J. Rare Earths* **41**, 182 (2023).

[10] C.K. Jørgensen, in: *Handbook on the Physics and Chemistry of Rare Earths*, Vol. 11, 1988, Ch. 75, p. 197.

[11] S.-L. Liu, H.-R. Fan, X. Liu, J. Meng, A.R. Butcher, L. Yann, K.-F. Yang, X.-C. Li, *Ore Geol. Rev.* **157**, 105428 (2023).

[12] J. Merle, *Monazite deposits of the southeastern Atlantic States*, USGS, 1953.

[13] D.R. Lide, *CRC Handbook of Chemistry and Physics*, 90th ed. CRC Press/Taylor and Francis, Boca Raton (FL) 2010.

[14] M.F. de Campos, in: *Proc. of the 25th Int. Workshop on Rare Earth Permanent Magnets and Advanced Magnetic Materials and Their Applications (REPM 2018)*, Beijing 2018, A0400-01.

[15] M. de Carvalho, *Projeto Caldeira — Desenvolvendo o Depósito de ETR de Maior Teor no Mundo*, 2013.

[16] S.B. Castor, *Can. Mineral.* **46**, 779 (2008).

[17] SEC Technical Report Summary, Pre-Feasibility Study Mountain Pass Mine, San Bernardino County (CA), SRK Consulting, 2022.

[18] P. Hellman, *Rare Earths Assessment of Ionic Adsorbed Deposits*, 2023.

[19] J.Y. Galarza, J. Meléndez, A. Karakas, M. Asplund, D. Lorenzo-Oliveira, *Mon. Not. R. Astron. Soc. Lett.* **502**, L104 (2021).

[20] X. Guangxian, X. Jimei *New Frontiers in Rare Earth Science and Applications: Proceedings of the International Conference on Rare Earth Development and Applications, Beijing, 1985.* Academic Press Inc, 1985.

[21] X. Wang, K. Huang, W. Cao, P. Sun, N. Sui, W. Song, H. Liu, *J. Rare Earths* **38**, 203 (2020).

[22] V.V. Belova, *Theor. Found. Chem. Eng.* **51**, 599 (2017).

[23] S. Gao, *Inorg. Chem. Front.* **8**, 10 (2021).

[24] J. Lucas, P. Lucas, T. Le Mercier, A. Rollat, W.G. Davenport, *Rare Earths: Science, Technology, Production and Use*, Elsevier, 2014.

[25] Z. Chen, Y.K. Lim, D. Brown, *IEEE Trans. Magn.* **51**, 2102104 (2015).

[26] J.F. Herbst, M.S. Meyer, F.E. Pinkerton, *J. Appl. Phys.* **111**, 07A718 (2012).

[27] B. Zhou, Y. Liu, S. Li, W. Fan, X. Liao, J. He, H. Yu, Z. Liu, *J. Rare Earths* **41**, 1058 (2023).

[28] S. Hirosawa, Y. Matsuura, H. Yamamoto, S. Fujimura, M. Sagawa, H. Yamauchi, *J. Appl. Phys.* **59**, 873 (1986).

[29] J.F. Herbst, *Rev. Mod. Phys.* **63**, 819 (1991).

[30] E.A. Périgo, I. Titov, R. Weber, D. Honecker, E.P. Gilbert, M.F. de Campos, A. Michels, *J. Alloys Compd.* **677**, 139 (2016).

[31] M.F. de Campos, F.A. Sampaio da Silva, S.A. Romero, J.A. de Castro, in: *14th Int. Symp. on Linear Drivers for Industry Applications (LDIA)*, 2023.

[32] B.D. Cullity, C.D. Graham Jr., *Introduction to Magnetic Materials*, 2nd ed., Wiley, Hoboken (NJ) 2009.

[33] M.F. de Campos, J.A. de Castro *J. Rare Earths* **37**, 1015 (2019).

[34] M.F.de Campos, *Mater. Sci. Forum* **869**, 591 (2016).

[35] S. Munro, *Comparing 10 Leading EV Motors* (free webcast), 2020.

[36] M.F. de Campos, J.A. de Castro, in: 2019-Sustainable Industrial Processing Summit, Vol. 13, 2019, p. 103.

[37] R. Thomas, H. Husson, L. Garbuio, L. Gerbaud, in: 17th Int. Conf. on Electrical Machines, Drives and Power Systems (ELMA), Sofia 2021.

[38] S. Jurkovic, K. Rahman, B. Bae, N. Patel, P. Savagian, in: *2015 IEEE Energy Conversion Congress and Exposition (ECCE)*, IEEE, 2015.

[39] Q. Ma, A. El Refaie, B. Lequesne, *IEEE Trans. Ind. Appl.* **56**, 1452 (2020).

[40] J. Frevert, in: KMT 2022; 13. GMM/ETG-Symposium, Linz, 2022.

[41] J.R. Hendershot, Electric Traction Machine Choices for Hybrid & Electric Vehicles, Florida International University, 2014.

[42] E. Dalla, Low Cogging Torque, "High Torque Density Traction Motor", US Patent 2020/0127508 A1, 2020.

[43] L.E. Olsen, D. Nelson, K. Laskaris, H. Ge, E. Filip, C. Vega, P. Pellerey, V. Papanikolaou, "Permanent Magnet Motor with Wrapping", World Patent WO2021225902A1, 2021.

[44] J. Binder, M. Silvagni, S. Ferrari, B. Deusinger, A. Tonoli, G. Pellegrino, in: *2023 IEEE Workshop on Electrical Machines Design, Control and Diagnosis (WEMDCD)*, 2023.

[45] M. Clauer, A. Binder, *Elektrotech. Inftech.* **140**, 302 (2023).

[46] A. Bensalah, G. Barakat, Y. Amara, *Energies* **15**, 6700 (2022).

[47] G.E. Barter, L. Sethuraman, P. Bortolotti, J. Keller, D.A. Torrey, *Appl. Energy* **344**, 121272 (2023).

[48] E.C. Stoner, E.P. Wohlfarth, *IEEE Trans. Magn.* **27**, 3475 (1991).

[49] M.F de Campos, J.A de Castro, *Acta Phys. Pol. A* **136**, 737 (2019).

[50] F.E. Luborsky, *J. Appl. Phys.* **37**, 1091 (1966).

[51] M.F. de Campos, S.A. Romero, D. Rodrigues, *Mater. Sci. Forum* **881**, 128 (2016).

[52] M. Mehedi, Ph.D. Thesis, University of Minnesota, Twin Cities, 2018.

[53] D. Liang, W. Yang, X. Wang et al., *AIP Adv.* **13**, 025104 (2023).

[54] J. Cui, M. Kramer, L. Zhou, F. Liu, A. Gabay, G. Hadjipanayis, B. Balasubramanian, D. Sellmyer, *Acta Mater.* **158**, 118 (2018).

[55] J. Ormerod, A. Karati, A.P.S. Baghel, D. Prodius, I.C. Nlebedim, *Sustainability* **15**, 14901 (2023).

[56] E.P. Wohlfarth, *Adv. Phys.* **8**, 87 (1959).

[57] E.C. Stoner, *Rep. Prog. Phys.* **13**, 83 (1950).

[58] W. Hosford, *Physical Metallurgy*, 2nd ed., CRC Press, 2010.

[59] A. Perrin, S. McCall, M. McElfresh, D.E. Laughlin, M.E. McHenry, *J. Phase Equilib. Diffus.* **42**, 617 (2021).

[60] S. Tavares, K. Yang, M.A. Meyers, *Prog. Mater. Sci.* **132**, 101017 (2023).

[61] C. Zhou, M. Pan, *Int. J. Electrochem. Sci.* **14**, 10387 (2019).

[62] A.J.J. Koch, P. Hokkeling, M.G. von der Steeg, K.J. de Vos, *J. Appl. Phys.* **31**, S75 (1960).

[63] Z. Abdelnour, H. Mildrum, K. Strnat, *IEEE Trans. Magn.* **17**, 2651 (1981).

[64] S.A. Romero, D. Rodrigues Jr., T. Germano, R. Cohen, J.A. de Castro, M.F. de Campos, *Appl. Nanosci.* **13**, 6353 (2023).

[65] S.A. Romero, A.J. Moreira, F.F.G. Landgraf, M.F. de Campos, *J. Magn. Magn. Mater.* **514**, 167147 (2020).

[66] S. Constantinides, "Manufacture of Modern Permanent Magnet Materials", 2014.

[67] V. Chaudhary, R. Ramanujan, *Sci. Rep.* **6**, 35156 (2016).

[68] E. Burzo, *Rom. Rep. Phys.* **63**, Supplement, 1316 (2011).

[69] J. Kitagawa, K. Sakaguchi, T. Hara, F. Hirano, N. Shirakawa, M. Tsubota, *Metals* **10**, 1644 (2020).